J. Austral. Math. Soc. Ser. B 27 (1986), 327–345

AIRFOILS MOVING IN AIR CLOSE TO A DYNAMIC WATER SURFACE

I. H. GRUNDY[1]

(Received 3 April 1985; revised 15 May 1985)

Abstract

Steady potential flow about a thin wing, flying in air above a dynamic water surface, is analysed in the asymptotic limit as the clearance-to-length ratio tends to zero. This leads to a non-linear integral equation for the one-dimensional pressure distribution beneath the wing, which is solved numerically. Results are compared with established "rigid-ground" and "hydrostatic" theories. Short waves lead to complications, including non-uniqueness, in some parameter ranges.

1. Introduction

Wings flying in close proximity to the ground, that is, in extreme ground effect, have been studied by a number of authors, e.g. Tuck [5], [6], Strand, Royce and Fujita [3], and Widnall and Barrows [11]. These authors have recognized that the prevailing two-dimensional flow (steady or otherwise) becomes approximately one-dimensional in the small gap between the wing and the (rigid) ground. A common result is that the pressure in the gap varies as the negative inverse square of the clearance. The constant of proportionality here is determined by applying the Kutta, or smooth-detachment, condition at the trailing edge. Hence, if the trailing edge is the closest point to the ground, positive lift results. In fact, near-stagnation pressure is attainable in the gap, producing lift many times greater than that experienced out of ground effect.

Recently, Tuck [8] has replaced the rigid ground plane by a free-surface of water which deforms hydrostatically in response to the pressure in the gap. The result is a cubic equation for the gap pressure, which is easily solved. Tuck displays results at various values of the sole parameter, namely a Froude number based on the trailing edge height. Features of the solution include increased lift

[1]Department of Applied Mathematics, The University of Adelaide, Adelaide, South Australia, 5000.

due to the static depression of the free-surface under the airfoil, and step discontinuities (in general) in the pressure distribution and free-surface displacement at the leading edge.

The effect of the hydrostatic assumption is to neglect the motion of the water resulting from the disturbance. Some justification for this assumption follows from Tuck [4]. Briefly, the air velocity is assumed large enough so that the dynamic contribution to the pressure in the air is much greater than that in the water. There is a delicate balance, however. The air/water density ratio must also be small enough so that the disturbance to the water motion is negligible.

In this paper we take the view that the disturbance to the water motion, although small, is not negligible. That is, we consider a true hydrodynamic model for the free-surface. We proceed on the assumption that the slope of the free-surface is small everywhere (except perhaps at the leading edge, where in general, we expect a pressure jump). We are thus able to linearize the free-surface boundary condition.

The free-surface displacement caused by a pressure distribution acting on a uniform stream is well known in connection with linearized planing-surface theory, and can be written as an integral of the pressure and a known kernel. See Lamb [2], Wehausen and Laitone [10], and Tuck [7]. It is a simple matter then, to combine the aerodynamic "channel-flow" and hydrodynamic "free-surface" contributions to form a non-linear integral equation for the gap pressure. This integral equation is not only parameterized by the Froude number based on height, but also by a second Froude number, based on the airfoil length, which we denote by F_L.

We present a successful numerical scheme for the solution of this integral equation, and display results for some simple airfoil shapes at various values of the two Froude numbers. At moderate to high values of F_L, that is, in the regime in which we expect practical vehicles to operate, it is found that the pressure distributions and lift coefficients approach those obtained over rigid ground.

We ask, "In what limit, if any, do the results of our hydrodynamic theory approach those of the hydrostatic theory?". The obvious limit is that as F_L tends to zero, indicating a weakening of hydrodynamic effects. However, things are complicated by the presence of short waves in the hydrodynamic model as F_L decreases. We can divide the various airfoil shapes into two categories, namely, those whose pressure distribution in the hydrostatic theory is continuous, particularly at the leading edge, and those whose pressure distribution is not. Those in the first category produce short waves in the hydrodynamic theory, whose amplitude also diminishes as F_L tends to zero. Those in the second category produce short waves which persist, as a direct result of the pressure jump, in the low-F_L limit. Thus the hydrostatic and hydrodynamic theories *do not* agree in any limit for a wide range of airfoil shapes!

Or do they? One might argue that discontinuities in the pressure distribution are not physically acceptable, and that the gap solution requires some matching to a local leading edge expansion as, say, in Tuck and Bentwich [9]. Such smoothing would then be critical, as we have seen above, to the formation of waves in the low-F_L limit. At the same time, however, this smoothing would be effective in a region of ever-decreasing size, tending to zero with F_L. It might also be argued that, as a result of the short waves, the linearization of the free-boundary condition must fail in the low-F_L limit. Indeed, some evidence for this is apparent in the loss of numerical accuracy and the presence of multiple solutions (indicating unstable solutions?), in this limit.

In any case, it is clear that the low-F_L limit requires more attention than the scope of the present paper allows.

2. Problem formulation

We assume steady, two-dimensional, irrotational flow of an incompressible fluid (e.g. air at low Mach number) of density ρ_A, over a free surface of another incompressible fluid (e.g. water) of density ρ_W, relative to a thin airfoil of length L, fixed between $x^* = 0$ and $x^* = L$. (See Figure 1.)

We let the lower surface of the airfoil be given by $y^* = h^*(x^*)$, the upper surface by $y^* = h^{+*}(x^*)$, and the air-water interface by $y^* = \eta^*(x^*)$. The airfoil is always close to the plane $y^* = 0$, (i.e. to the undisturbed free surface height at infinity) and the disturbance to the uniform stream is comparable to a measure of

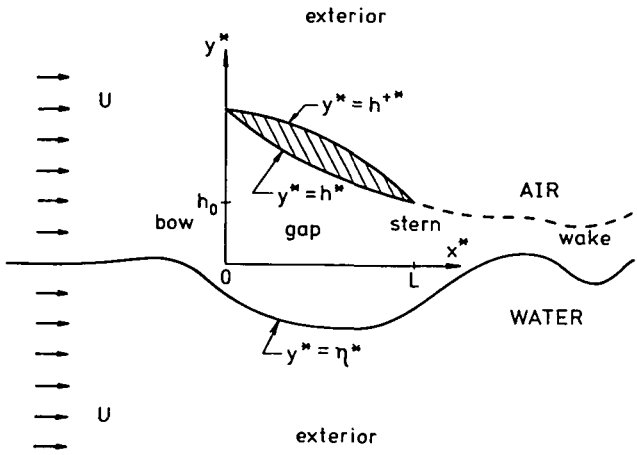

Figure 1. Sketch of flow geometry.

https://doi.org/10.1017/S0334270000004963 Published online by Cambridge University Press

$h^*(x^*)$, say h_0, the trailing edge height. That is,

$$\eta^*,\ h^*,\ h^{+*} = O(h_0). \tag{2.1}$$

We assume $h_0 \ll L$, thus introducing a small parameter

$$\varepsilon = h_0/L. \tag{2.2}$$

Our aim is to seek asymptotic expansions, as $\varepsilon \to 0$, of $\phi^*(x^*, y^*)$, and $\Phi^*(x^*, y^*)$, the unscaled velocity potentials in the air and water respectively.

In each of the air and water regions we must solve Laplace's equation for the velocity potential with appropriate boundary conditions. In the air we must solve

$$\frac{\partial^2\phi^*}{\partial x^{*2}} + \frac{\partial^2\phi^*}{\partial y^{*2}} = 0, \tag{2.3}$$

subject to the kinematic condition, that no fluid crosses the boundaries, η^*, h^* and h^{+*}. That is,

$$\frac{\partial\phi^*}{\partial y^*} = \frac{\partial\phi^*}{\partial x^*}\frac{\partial h^*}{\partial x^*} \quad \text{on } y^* = h^*(x^*), \tag{2.4}$$

$$\frac{\partial\phi^*}{\partial y^*} = \frac{\partial\phi^*}{\partial x^*}\frac{\partial h^{+*}}{\partial x^*} \quad \text{on } y^* = h^{+*}(x^*) \tag{2.5}$$

and

$$\frac{\partial\phi^*}{\partial y^*} = \frac{\partial\phi^*}{\partial x^*}\frac{\partial\eta^*}{\partial x^*} \quad \text{on } y^* = \eta^*(x^*). \tag{2.6}$$

The flow must also approach a uniform stream at infinity, i.e.

$$\phi^* \to Ux^* \quad \text{as } x^{*2} + y^{*2} \to \infty. \tag{2.7}$$

In the water we must similarly solve

$$\frac{\partial^2\Phi^*}{\partial x^{*2}} + \frac{\partial^2\Phi^*}{\partial y^{*2}} = 0, \tag{2.8}$$

subject to

$$\frac{\partial\Phi^*}{\partial y^*} = \frac{\partial\Phi^*}{\partial x^*}\frac{\partial\eta^*}{\partial x^*} \quad \text{on } y^* = \eta^*(x^*) \tag{2.9}$$

and

$$\Phi^* \to Ux^* \quad \text{as } x^{*2} + y^{*2} \to \infty. \tag{2.10}$$

To determine the unknown shape of the free surface $y^* = \eta^*(x^*)$, one further boundary condition, expressing continuity of pressure across the air-water interface, is required. If we let $p_A(x^*, y^*)$ and $p_W(x^*, y^*)$ be the air and water

https://doi.org/10.1017/S0334270000004963 Published online by Cambridge University Press

pressures respectively, this equation is simply

$$p_A(x^*, \eta^* + 0) = p_W(x^*, \eta^* - 0), \tag{2.11}$$

where p_A and p_W are calculated from Bernoulli's equation for steady, incompressible, irrotational flow.

Also associated with the flow around the airfoil, is a trailing vortex sheet or wake, emanating from the trailing edge of the airfoil. We denote this wake by

$$y^* = h_w^*(x^*), \qquad x^* \geqslant L. \tag{2.12}$$

The kinematic condition

$$\frac{\partial \phi^*}{\partial y^*} = \frac{\partial \phi^*}{\partial x^*} \frac{\partial h_w^*}{\partial x^*} \tag{2.13}$$

holds on the wake, as it does on the body. We can, if we wish, determine h_w^* from continuity of pressure across the wake, in much the same way as we determine η^*, i.e.

$$p_A(x^*, h_w^* + 0) = p_A(x^*, h_w^* - 0). \tag{2.14}$$

For our purposes, however, it is sufficient to note that if we let $x^* \to L^+$, (2.14) defines the Kutta condition at the trailing edge.

3. Asymptotic solution

We divide the flow region into five subregions as $\varepsilon \to 0$. These, as shown in Figure 1, are

(a) the exterior E: $x^* = O(L)$, $y^* = O(L)$

(b) the gap G: $x^* = O(L)$, $y^* = O(h_0)$, $0 < x^* < L$,

(c) the wake W: $x^* = O(L)$, $y^* = O(h_0)$, $x^* > L$,

(d) the bow B: $x^* = O(h_0)$, $y^* = O(h_0)$,

(e) the stern S: $x^* - L = O(h_0)$, $y^* = O(h_0)$.

It is clear from a formal asymptotic analysis of the exterior and wake, that the flow there is a small perturbation of the incident uniform stream, i.e.

$$\phi^* = Ux^* + O(\varepsilon L)$$

and

$$\Phi^* = Ux^* + O(\varepsilon L). \tag{3.1}$$

https://doi.org/10.1017/S0334270000004963 Published online by Cambridge University Press

Looking back to the previous section, and in particular to equation (2.14), this means that the flow must approach free stream conditions at the exit to the gap.

Within the gap, however, the flow is *not* a small perturbation of the uniform stream, and this flow is of primary importance in estimating forces etc. on the body. To obtain the correct equations to be satisfied in this region, we define the following scaled independent variables

$$X = x^*/L, \qquad Y = y^*/h_0, \tag{3.2}$$

and dependent variables

$$\phi(X,Y) = \phi^*(x^*, y^*)/(UL), \quad \Phi(X,Y) = \Phi^*(x^*, y^*)/(UL),$$
$$h(X) = \frac{h^*(x^*)}{h_0}, \quad h^+(X) = \frac{h^{+*}(x^*)}{h_0}, \quad \eta(X) = \frac{\eta^*(x^*)}{h_0}. \tag{3.3}$$

We assume that the air-water density ratio, ρ_A/ρ_W, is small, specifically $O(\varepsilon)$, and we define the corresponding scaled density ratio ρ by

$$\rho\varepsilon = \rho_A/\rho_W, \tag{3.4}$$

where ρ is an $O(1)$ quantity. It is convenient to define two Froude numbers, namely

$$F_L = \left(U^2/(gL)\right)^{1/2}, \tag{3.5}$$

which is the usual Froude number based on length, and a specially scaled Froude number, namely

$$F_h = \left(U^2\rho_A/(\rho_W g h_0)\right)^{1/2} = \sqrt{\rho}\, F_L, \tag{3.6}$$

which is based on the trailing edge height, and which appears in Tuck [8]. We assume that both F_L and F_H are $O(1)$ quantities.

We expand the unknowns ϕ, Φ and η in powers of the small parameter ε; thus

$$\phi(X,Y) = \phi_0(X,Y) + \varepsilon\phi_1(X,Y) + \varepsilon^2\phi_2(X,Y) + \cdots, \tag{3.7}$$

$$\Phi(X,Y) = \Phi_0(X,Y) + \varepsilon\Phi_1(X,Y) + \varepsilon^2\Phi_2(X,Y) + \cdots, \tag{3.8}$$

and

$$\eta(X) = \eta_0(X) + \varepsilon\eta_1(X) + \varepsilon^2\eta_2(X) + \cdots. \tag{3.9}$$

We then rewrite (2.3) to (2.12) in terms of the scaled variables.

Laplace's equation, in the air, becomes

$$\varepsilon^2\frac{\partial^2\phi}{\partial X^2} + \frac{\partial^2\phi}{\partial Y^2} = 0, \tag{3.10}$$

subject to

$$\frac{\partial\phi}{\partial Y} = \varepsilon^2\frac{\partial\phi}{\partial X}\frac{\partial\eta}{\partial X} \quad \text{on } Y = \eta(X), \tag{3.11}$$

https://doi.org/10.1017/S0334270000004963 Published online by Cambridge University Press

and

$$\frac{\partial \phi}{\partial Y} = \varepsilon^2 \frac{\partial \phi}{\partial X} \frac{\partial h}{\partial X} \quad \text{on } Y = h(X). \tag{3.12}$$

Conditions (2.5), (2.7) and (2.13) do not apply directly to the gap but can be recovered by matching with regions (a), (c), (d) and (e) at a later stage if necessary.

We now substitute our asymptotic expansions for ϕ and η into (3.10) to (3.12). Equations (3.10) and (3.11) are satisfied if

$$\phi_0 = \phi_0(X), \tag{3.13}$$

$$\phi_1 = \phi_1(X), \tag{3.14}$$

and

$$\phi_2(X, Y) = \phi_2(X, 0) + Y \frac{d}{dX}\left\{ \eta_0(X) \frac{d}{dX}\phi_0(X) \right\} - \frac{1}{2} Y^2 \frac{d^2}{dX^2}\phi_0(X). \tag{3.15}$$

Equation (3.12) is then satisfied if

$$(h(X) - \eta_0(X)) \frac{d}{dX}\phi_0(X) = \text{constant} \tag{3.16}$$

holds throughout the gap region, that is, if we have classical one-dimensional, or channel, flow.

Similarly, Laplace's equation in the water becomes

$$\varepsilon^2 \frac{\partial^2 \Phi}{\partial X^2} + \frac{\partial^2 \Phi}{\partial Y^2} = 0, \tag{3.17}$$

subject to

$$\frac{\partial \Phi}{\partial Y} = \varepsilon^2 \frac{\partial \Phi}{\partial X} \frac{\partial \eta}{\partial X} \quad \text{on } Y = \eta. \tag{3.18}$$

Here, we note that in (3.11) and (3.18) we have made our linearized-free-surface assumption. That is, the slope of $Y = \eta$ is assumed to be a quantity of $O(\varepsilon)$ magnitude.

Substitution of (3.8) and (3.9) into (3.17) and (3.18) leads to

$$\Phi_0 = \Phi_0(X), \tag{3.19}$$

$$\Phi_1 = \Phi_1(X), \tag{3.20}$$

and

$$\Phi_2(X, Y) = \Phi_2(X, 0) + Y \frac{d}{dX}\left(\eta_0(X) \frac{d}{dX}\Phi_0(X) \right) - \frac{1}{2} Y^2 \frac{d^2}{dX^2}\Phi_0(X). \tag{3.21}$$

https://doi.org/10.1017/S0334270000004963 Published online by Cambridge University Press

This near-gap flow in the water can be matched immediately with the exterior flow at a great depth.

To accomplish this we define a scaled outer variable

$$y = y^*/L. \tag{3.22}$$

We also need to define a scaled velocity potential for the exterior water region, namely $\Psi(X, y)$. It is clear that Ψ will have the asymptotic form

$$\Psi(X, y) = X + \varepsilon\Psi_1(X, y) + \varepsilon^2\Psi_2(X, y) + \cdots \tag{3.23}$$

where $\Psi_1(X, y) \to 0$ as $X^2 + y^2 \to \infty$, except that, in accordance with the usual radiation condition, there may be a trailing sinusoidal wave on $y = 0$ as $X \to +\infty$. Now Ψ, and hence Ψ_1, satisfies the full Laplace equation, there being no order ε^2 imbalance between the X and y derivative terms.

We match the "near-gap" and "exterior" regions by writing the inner expansion in terms of the outer variables, and equating coefficients of ε, obtaining

$$\Psi_0(X, 0^-) = X = \Phi_0(X), \tag{3.24}$$

$$\Psi_1(X, 0^-) = \Phi_1(X), \tag{3.25}$$

and

$$\frac{d\Psi_1}{dy}(X, 0^-) = \frac{d}{dX}\eta_0(X). \tag{3.26}$$

As we shall see later, it is profitable to concentrate on a solution for Ψ instead of Φ.

We turn now to the pressure continuity condition on the free surface. Using Bernoulli's equation, p_A can be expressed in terms of ϕ^*. In unscaled form,

$$p_A + \rho_A g\eta^* + \frac{1}{2}\rho_A\left\{\left[\frac{\partial\phi^*}{\partial x^*}\right]^2 + \left[\frac{\partial\phi^*}{\partial y^*}\right]^2\right\} = p_0 + \frac{1}{2}\rho_A U^2. \tag{3.27}$$

Similarly, p_W is expressible in terms of Φ^*, namely

$$p_W + \rho_W g\eta^* + \frac{1}{2}\rho_W\left\{\left[\frac{\partial\Phi^*}{\partial x^*}\right]^2 + \left[\frac{\partial\Phi^*}{\partial y^*}\right]^2\right\} = p_0 + \frac{1}{2}\rho_W U^2 \tag{3.28}$$

where p_0 is the ambient or atmospheric pressure at infinity.

Using (3.27) and (3.28) we equate p_A and p_W and write the result in terms of non-dimensional variables, to obtain

$$\rho\eta\varepsilon^4 + \frac{1}{2}F_h^2\left[\frac{\partial\phi}{\partial X}\right]^2\varepsilon^3 + \frac{1}{2}F_h^2\left[\frac{\partial\phi}{\partial Y}\right]^2\varepsilon - \frac{1}{2}F_h^2\varepsilon^3$$
$$= \eta\varepsilon^3 + \frac{1}{2}F_L^2\left[\frac{\partial\Phi}{\partial X}\right]^2\varepsilon^2 + \frac{1}{2}F_L^2\left[\frac{\partial\Phi}{\partial Y}\right]^2 - \frac{1}{2}F_L^2\varepsilon^2 \quad \text{on } Y = \eta. \tag{3.29}$$

https://doi.org/10.1017/S0334270000004963 Published online by Cambridge University Press

We now substitute our asymptotic expansions for ϕ, Φ and η into (3.29) and apply this boundary condition on $Y = \eta_0(X)$. Conditions up to and including $O(\varepsilon^2)$ are satisfied already by

$$\phi_0 = \phi_0(X) \quad \text{and} \quad \Phi_0 = \Phi_0(X) = X.$$

The terms of $O(\varepsilon^3)$ provide more interest, however, demanding that

$$\eta_0(X) = \frac{1}{2}F_h^2\left\{\left[\frac{d\phi_0}{dX}\right]^2 - 1\right\} - F_L^2\frac{d\Phi_1}{dX} \tag{3.30}$$

be satisfied on $Y = \eta_0(X)$.

We note that (3.30) without the last term on the right hand side, namely

$$\eta_0(X) = \frac{1}{2}F_h^2\left\{\left[\frac{d\phi_0}{dX}\right]^2 - 1\right\}, \tag{3.31}$$

is the boundary condition obtained in the hydrostatic theory of Tuck [8]. This indicates that in certain circumstances, the hydrodynamic results may approach those of the hydrostatic theory as $F_L \to 0$.

Returning to (3.30), we are able to substitute (3.25) into this equation to obtain

$$\eta_0(X) = -\frac{1}{2}F_h^2P(X) - F_L^2\frac{\partial\Psi_1}{\partial X}(X,0^-), \tag{3.32}$$

where

$$P(X) = 1 - \left[\frac{d}{dX}\phi_0(X)\right]^2. \tag{3.33}$$

Differentiating once, and using (3.26), we obtain

$$\frac{\partial\Psi_1}{\partial y}(X,0^-) + F_L^2\frac{\partial^2\Psi_1}{\partial X^2}(X,0^-) = -\frac{1}{2}F_h^2\frac{d}{dX}P(X). \tag{3.34}$$

The flow in the air is to leading order a uniform stream outside the gap, that is, $\phi_0(X) = X$, hence the right hand side of equation (3.34) is zero everywhere but in the gap.

We now have a complete boundary value problem for Ψ_1, namely,

$$\frac{\partial^2\Psi_1}{\partial X^2} + \frac{\partial^2\Psi_1}{\partial y^2} = 0 \tag{3.35}$$

in the lower half plane, subject to

$$\frac{\partial\Psi_1}{\partial y} + F_L^2\frac{\partial^2\Psi_1}{\partial X^2} = \begin{cases} -\frac{1}{2}F_h^2\frac{d}{dX}P(X), & 0 < X \leqslant 1, \\ 0, & \text{elsewhere,} \end{cases} \tag{3.36}$$

https://doi.org/10.1017/S0334270000004963 Published online by Cambridge University Press

on $y = 0$, and

$$\Psi_1 \to 0 \quad \text{as } X^2 + y^2 \to \infty, \tag{3.37}$$

subject to the radiation condition as before.

4. Integral equation

The boundary value problem for Ψ_1 is well known from linearized planing-surface theory, and can be solved easily for example by Fourier transform or complex variable methods. (See Tuck [7], Lamb [2], Wehausen and Laitone [10].)

It follows from this purely hydrodynamic solution for Ψ_1, that the free surface displacement caused by the pressure distribution beneath the airfoil acting on the water, is given by

$$\eta_0(X) = \frac{1}{2}F_h^2/F_L^2 \int_0^1 P(\xi) K_0'[\gamma(X - \xi)]\, d\xi \tag{4.1}$$

where

$$\gamma = 1/F_L^2, \tag{4.2}$$

$$K_0(u) = -\frac{1}{\pi} f(u) + \begin{cases} 2\cos u - 1, & u > 0, \\ 0, & u < 0, \end{cases} \tag{4.3}$$

and

$$f(u) = Ci(|u|)\sin u - si(|u|)\cos u \operatorname{sgn} u \tag{4.4}$$

is the auxiliary function for the sine and cosine integrals, Abramowitz and Stegun [1]. In contrast to the hydrostatic theory, $\eta_0(X)$, as given by (4.1), is continuous, even for step-function discontinuities in $P(X)$.

Another expression linking the free surface displacement to the gap pressure distribution is the "one-dimensional continuity" equation, (3.16), which follows from aerodynamic considerations only. We rearrange (3.16), using (3.33), to obtain

$$\eta_0(X) = h(X) - [1 - \eta_0(1)]/\sqrt{(1 - P(X))}\,. \tag{4.5}$$

The constant, $1 - \eta_0(1)$, is chosen so as to enforce the Kutta condition, $P(1) = 0$, at the trailing edge.

Combining (4.1) and (4.5) by the elimination of $\eta_0(X)$ gives the following non-linear integral equation for $P(X)$,

$$h(X) = [1 - \eta_0(1)]/\sqrt{(1 - P(X))} + \frac{1}{2}F_h^2/F_L^2 \int_0^1 P(\xi) K_0'[\gamma(X - \xi)]\, d\xi. \tag{4.6}$$

https://doi.org/10.1017/S0334270000004963 Published online by Cambridge University Press

The integral on the right-hand side of (4.6) allows the formation of waves of wavelength $2\pi F_L^2$. Any such waves become shorter and shorter as the Froude number, F_L, tends to zero; the question of whether or not their amplitude also tends to zero in this limit is considered later. Note that the hydrostatic theory of Tuck [8] has no such waves.

If we let F_L tend to infinity, i.e. $\gamma \to 0$, with F_h fixed, we can replace $K_0'(u)$ in (4.6) by its leading order approximation, that is,

$$K_0'(u) \sim -\frac{1}{\pi} \log|u| \quad \text{as } u \to 0. \tag{4.7}$$

It follows that $\eta_0 \sim 0(\gamma \log \gamma)$ as $\gamma \to 0$. That is, in this limit, the integral term in (4.6) tends to zero and the pressure $P(X)$ approaches that for a rigid ground plane.

5. Numerical method

We divide the region under the body $[0, 1]$ into N subintervals

$$I_j = (S_{j-1}, S_j), \qquad j = 1, 2, \ldots, N, \tag{5.1}$$

where $S_0 = 0$ and $S_N = 1$. In practice, a uniform grid is satisfactory. We let the midpoint of I_j be

$$X_j = \frac{S_{j-1} + S_j}{2}, \qquad j = 1, 2, \ldots, N. \tag{5.2}$$

We then approximate the unknown pressure distribution $P(X)$ by assuming it to be a step function, i.e.

$$P(X) = P(X_j) = P_j, \qquad X \in I_j, \qquad j = 1, 2, \ldots, N. \tag{5.3}$$

Similarly, we assume the known underbody shape $h(X)$ acts through the midpoints of I_j, i.e.

$$h(X) = h(X_j) = h_j, \qquad X \in I_j, \qquad j = 1, 2, \ldots, N. \tag{5.4}$$

We can then discretize (4.6) accordingly, to obtain

$$h_i = [1 - \eta_0]/\sqrt{(1 - P_i)} + \sum_{j=1}^{N} A_{ij} P_j, \qquad i = 1, 2, \ldots, N, \tag{5.5}$$

where $\eta_0 = \eta_0(1)$ and

$$A_{ij} = \frac{1}{2} F_h^2 \left[K_0\left[\gamma(X_i - S_{j-1})\right] - K_0\left[\gamma(X_i - S_j)\right] \right], \quad \forall\, i, j. \tag{5.6}$$

https://doi.org/10.1017/S0334270000004963 Published online by Cambridge University Press

We now solve the set of non-linear algebraic equations (5.5), using Newton iterations. If η_0^0 is an initial guess for η_0, and P_i^0 is an initial guess for P_i, we obtain

$$d_i = b_i\eta_0 + c_iP_i + \sum_{j=1}^{N} A_{ij}P_j, \tag{5.7}$$

where

$$d_i = h_i - \left(1 - P_i^0\right)^{-1/2} + \frac{1}{2}\left(1 - \eta_0^0\right)P_i^0\left(1 - P_i^0\right)^{-3/2}, \tag{5.8}$$

$$b_i = -\left(1 - P_i^0\right)^{-1/2} \tag{5.9}$$

and

$$c_i = \frac{1}{2}\left(1 - \eta_0^0\right)\left(1 - P_i^0\right)^{-3/2}. \tag{5.10}$$

Notice that we have N equations in $N + 1$ unknowns, $\eta_0, P_1, P_2, \ldots, P_N$. We introduce our last equation, the Kutta condition, by assuming

$$P(X) \sim A(1 - X)^{1/2} \quad \text{as } X \to 1, \tag{5.11}$$

where A is a constant. This we apply at the points X_{N-1} and X_N to obtain

$$-\lambda P_{N-1} + P_N = 0, \tag{5.12}$$

where

$$\lambda = (1 - X_N)^{1/2}(1 - X_{N-1})^{-1/2}. \tag{5.13}$$

In matrix form we now have

$$CP = D \tag{5.14}$$

at each iteration, where

$$C = \begin{bmatrix} A_{11} + c_1 & A_{12} & \cdots & A_{1N-1} & A_{1N} & b_1 \\ A_{21} & A_{22} + c_2 & \cdots & A_{2N-1} & A_{2N} & b_2 \\ \vdots & \vdots & & \vdots & \vdots & \vdots \\ A_{N1} & A_{N2} & \cdots & A_{NN-1} & A_{NN} + c_N & b_N \\ 0 & 0 & \cdots & -\lambda & 1 & 0 \end{bmatrix},$$

$$P = \begin{bmatrix} P_1 \\ P_2 \\ \vdots \\ P_N \\ \eta_0 \end{bmatrix}, \qquad D = \begin{bmatrix} d_1 \\ d_2 \\ \vdots \\ d_N \\ 0 \end{bmatrix}.$$

https://doi.org/10.1017/S0334270000004963 Published online by Cambridge University Press

We now solve the linear system (5.14), using a standard matrix inversion procedure, and iterate until a converged solution is obtained. Care must be taken to ensure that the initial guesses P_i^0 and η_0^0 are sufficiently good. Poor guesses can, after several iterations, produce values of P_i greater than unity, for which equations (5.8) to (5.10) fail to be meaningful. In particular, this problem occurs at low values of the Froude number F_L, where the character of the solution changes rapidly with small changes in F_L. By decreasing F_L in small steps, and using the converged solution at the previous F_L value as an initial guess for the solution at the next value, we can often avoid such problems.

Apart from these initial-guess problems, the matrix inversion is usually straightforward, and convergence occurs quickly. Four or five iterations are usually sufficient. Good results (accurate to three decimal places) are obtainable with $N = 50$, except in the short wave ($F_L \leqslant 0.2$) régime, where accuracy gradually decreases with F_L.

6. Numerical results

(a) Low Froude numbers

As mentioned previously, we are interested in the question of whether the hydrodynamic results might agree with the hydrostatic theory in some limit. Equation (3.30) suggests this may be possible by letting F_L appoach zero, keeping F_h fixed.

Our numerical evidence suggests, however, that the hydrostatic theory is approached in the low-F_L limit only for a certain class of airfoil, namely those for which the hydrostatic theory predicts $P(0) = 0$, i.e. no pressure jump at the leading edge. This type of airfoil necessarily has leading and trailing edge heights equal.

On the other hand, the hydrostatic results do not appear to be recoverable for those bodies having a pressure jump at the leading edge. A jump such as this cannot be supported in the hydrodynamic theory without the formation of waves that persist as F_L tends to zero. The simplest example of an airfoil in this category is the flat-plate at positive angle of attack.

We ran the program to solve (4.6) using as input

$$h(X) = 1 + \alpha - \alpha X \tag{6.1}$$

for various values of F_L and α, at a typical value of F_h, namely $F_h = \sqrt{0.5}$. An output quantity of interest is the leading edge pressure $P(0)$. Figure 2 shows the behaviour of $P(0)$ for the flat-plate, at various α, for low values of F_L. The hydrostatic and rigid-ground limits are shown, for each α, as crosses on the left and right-hand sides respectively. Taking a typical example, namely $\alpha = 0.2$, we

https://doi.org/10.1017/S0334270000004963 Published online by Cambridge University Press

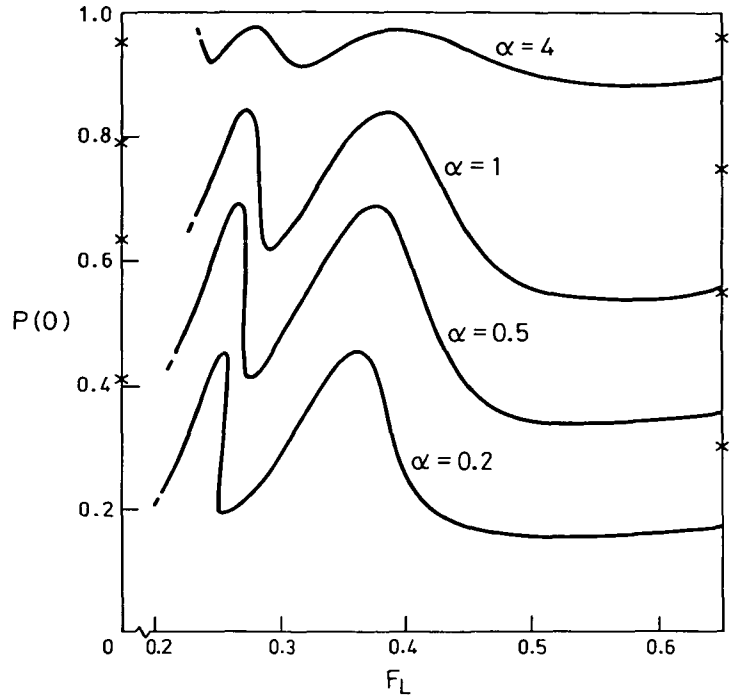

Figure 2. Leading edge pressure as a function of F_L, at $F_h = \sqrt{0.5}$, for the flat-plate at various values of the angle of attack α.

observe that $P(0)$ settles down to oscillate in the range 0.2 to 0.45 and shows no tendency either to approach zero, or to approach the hydrostatic value $P(0) = 0.41$. Figure 3 shows the behaviour of $P(X)$ for several values of F_L, at $\alpha = 0.2$.

We observe that the finite amplitude of the generated waves, as their wavelength shortens, prevents any approach to the hydrostatic limit.

Another striking feature of our output is that in some intervals of (low) F_L, the value of $P(0)$ is not unique. That is, the interaction between the pressure distribution and the shortening free-surface waves allows several different solutions for $P(X)$ to exist at a particular F_L. For example, as shown in Figure 4, for $\alpha = 0.2$ and $F_L = 0.25$, three distinct solutions exist, none of which appear to be unreasonable. This multiple solution phenomenon may suggest the onset of non-linear instability in the low-F_L domain, and it may indeed be that no stable solutions are possible below a certain F_L value.

In contrast to the flat-plate case, we *are* able to recover the hydrostatic results for bodies such as the fore-and-aft symmetric parabolic plate

$$h(X) = 1 + 4\alpha X(1 - X). \tag{6.2}$$

https://doi.org/10.1017/S0334270000004963 Published online by Cambridge University Press

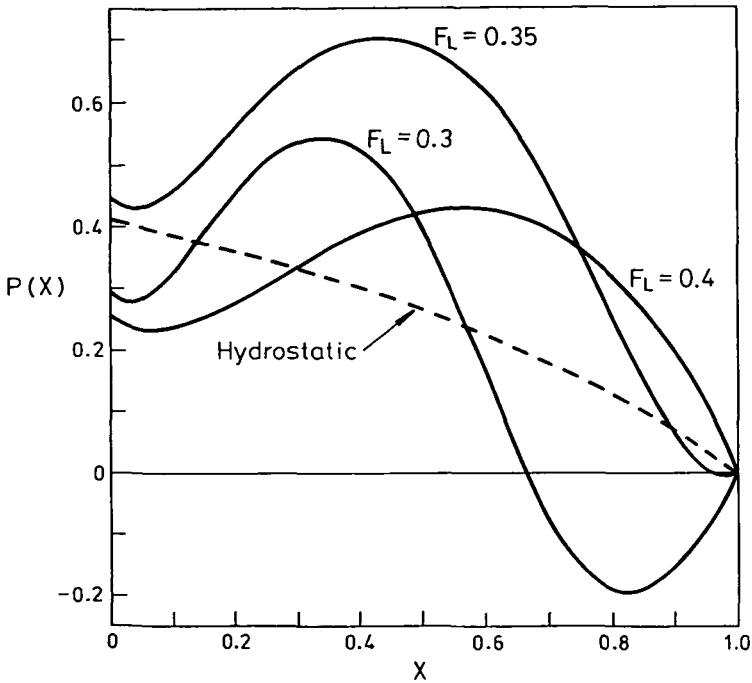

Figure 3. Pressure distribution for the flat-plate, at $\alpha = 0.2$ and $F_h = \sqrt{0.5}$, for various low values of F_L.

Figure 5 shows $P(0)$ in the low F_L domain, for $\alpha = 0.2$ and $F_h = 0.9$. It should be noted here that the dashed portion of the curve is speculative, with justification following from similar curves, not shown, at different values of F_h. As we might expect from the above, the approach to this limit is complicated by multiplicity of solutions below a certain value of F_L, namely 0.33. The general trend, however, seems to be that $P(0)$ tends to zero as F_L tends to zero, with any waves generated diminishing in amplitude as well as wavelength. Figure 6 shows some low-F_L parabolic-plate pressure distributions for which these waves appear to be disappearing.

(b) Higher values of F_L

Figure 7 shows the lift coefficient C_L, defined by

$$C_L = \int_0^1 P(X)\, dX, \tag{6.3}$$

for a range of values of F_L, for the flat-plate at $F_h = \sqrt{0.5}$ and $\alpha = 0.2$. Over this range, the lift coefficient varies from over twice that predicted by the hydrostatic theory to values, in some ranges, less than that predicted by the rigid-ground theory.

https://doi.org/10.1017/S0334270000004963 Published online by Cambridge University Press

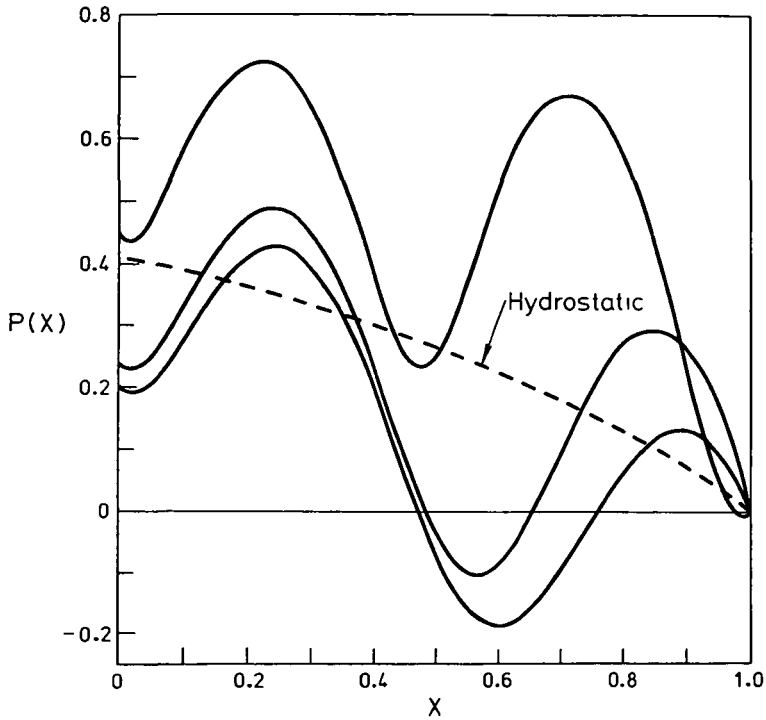

Figure 4. Three solutions for the flat-plate pressure distribution at $\alpha = 0.2$, $F_h = \sqrt{0.5}$ and $F_L = 0.25$.

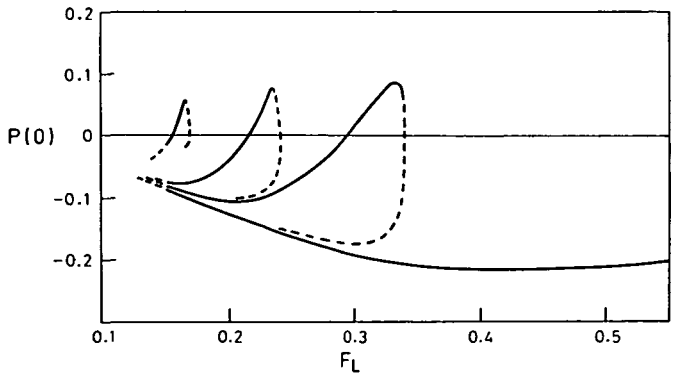

Figure 5. Leading edge pressure as a function of F_L, for the parabolic-plate at $\alpha = 0.2$ and $F_h = 0.9$.

https://doi.org/10.1017/S0334270000004963 Published online by Cambridge University Press

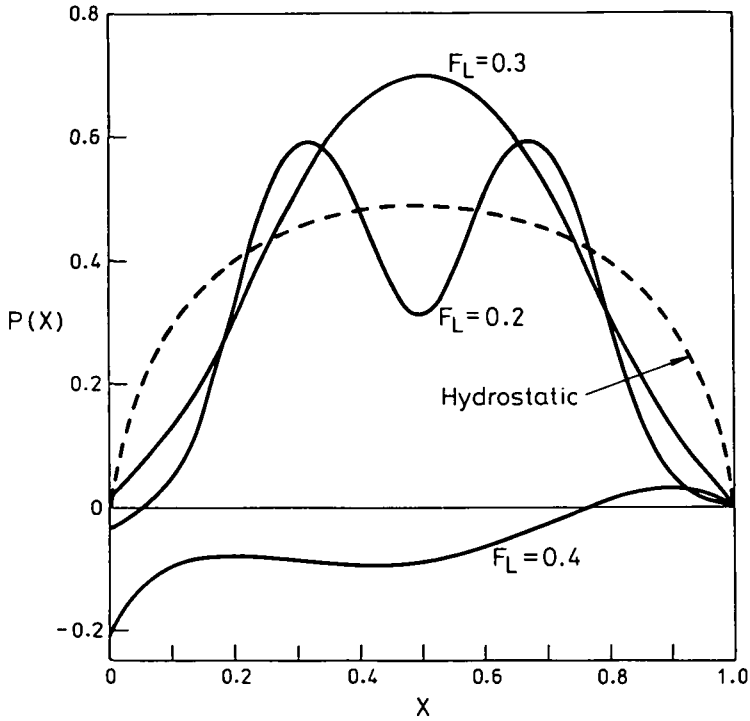

Figure 6. Pressure distribution for the parabolic-plate, at $\alpha = 0.2$ and $F_h = 0\,9$, for various low values of F_L.

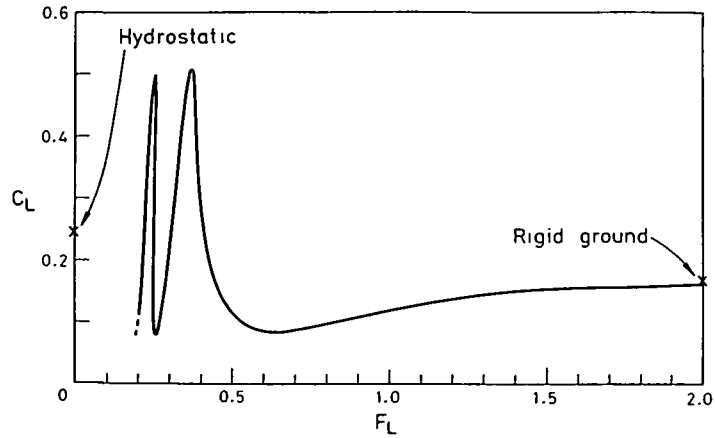

Figure 7 Lift coefficient as a function of F_L, for the flat-plate at $\alpha = 0\,2$ and $F_h = \sqrt{0.5}$.

https://doi.org/10.1017/S0334270000004963 Published online by Cambridge University Press

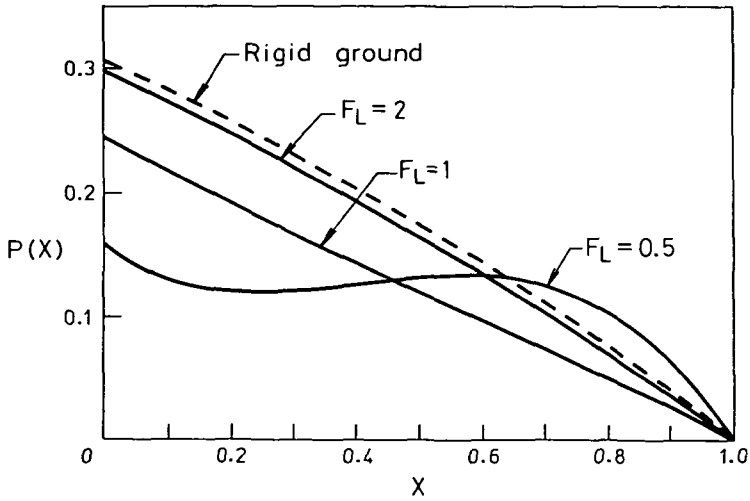

Figure 8. Pressure distribution for the flat-plate, at $\alpha = 0.2$ and $F_h = \sqrt{0.5}$, for various high values of F_L.

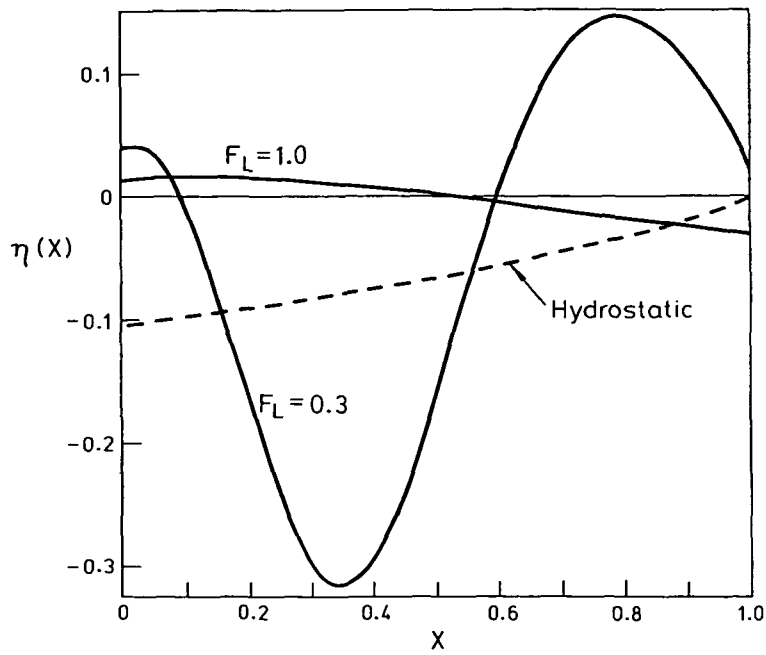

Figure 9. Free-surface displacement for the flat-plate at $\alpha = 0.2$ and $F_h = \sqrt{0.5}$, for $F_L = 0.3$ and 1.0.

https://doi.org/10.1017/S0334270000004963 Published online by Cambridge University Press

We expect that practical vehicles would tend to operate in the moderate to high F_L regime, ($F_L \geqslant 0.5$). For the flat-plate at these moderate to high F_L values, we observe that the lift coefficients obtained are below those predicted by the rigid-ground theory. Thus the effect of the water is to decrease lift. However, for sufficiently fast vehicles, e.g. $F_L \geqslant 2$, our computed results (Figure 8) show that lift is within 3% of that over rigid ground, and the pressure of the water can effectively be ignored.

Finally, Figure 9 shows flat-plate free-surface shapes for $F_L = 0.3$ and $F_L = 1.0$, compared to the hydrostatic result, at $\alpha = 0.2$ and $F_h = \sqrt{0.5}$. Typically the free-surface is always very close to the plane $Y = 0$ for high F_L, as is demonstrated by the $F_L = 1$ curve. Near the low F_L end of the spectrum, as we have noted previously and observe here, waves of relatively large amplitude prevent approach to the hydrostatic result.

References

[1] M. Abramowitz and I. A. Stegun (eds.), *Handbook of mathematical functions* (Dover, New York, 1964).

[2] H. Lamb, *Hydrodynamics* (Cambridge University Press, 1932).

[3] T. Strand, W. W. Royce and T. Fujita, "Cruise performance of channel-flow ground-effect machines", *J. Aero. Sci.* 29 (1962), 702–711

[4] E. O. Tuck, "On air flow over free surfaces of stationary water", *J. Austral. Math. Soc. Ser. B* 19 (1975), 66–80.

[5] E. O. Tuck, "A nonlinear unsteady one-dimensional theory for wings in extreme ground effect", *J. Fluid. Mech.* 98 (1980), 33–47.

[6] E. O. Tuck, "Steady flow and static stability of airfoils in extreme ground effect", *J. Eng. Math.* 15 (1981), 89–102.

[7] E. O. Tuck, "Linearized planing-surface theory with surface tension. Part I: Smooth detachment", *J. Austral. Math. Soc. Ser. B* 23 (1982), 241–258.

[8] E. O. Tuck, "A simple one-dimensional theory for air-supported vehicles over water", *J. Ship Re.* 28 (1984), 290–292.

[9] E. O. Tuck and M. Bentwich, "Sliding sheets: Lubrication with comparable viscous and inertia forces", *J. Fluid. Mech.* 135 (1983), 51–69.

[10] J. V Wehausen and E. V. Laitone, "Surface waves", in *Handbuch der Physik*, Vol. 9, (ed. S. Flugge), (Springer-Verlag, Berlin, 1960).

[11] S. E. Widnall and T. M Barrows, "An analytic solution for two- and three-dimensional wings in ground effect", *J. Fluid. Mech.* 41 (1970), 769–792.